December 8th, 2017

Final report for the project:

"Extent and Contributing Factors of Delayed Post-Fire Mortality in Glacier National Park"

Award Number: P14AC00855
Project Number: UCOB-104
Park/NPS Unit: Glacier NP
RM-CESU Cooperative Agreement Number: P14AC00749

Report prepared by:

Cameron E. Naficy
Geography Department, UCB 260,
University of Colorado,
Boulder, CO 80309
phone: (778) 834-7438
cameron.naficy@ubc.ca

Thomas T. Veblen
Geography Department, UCB 260,
University of Colorado,
Boulder, CO 80309
phone: (303) 492-8528
thomas.veblen@colorado.edu

Abstract

Field observations of areas burned within Glacier National Park (GNP) over the last twenty years suggest that substantial delayed post-fire tree mortality may be occurring in some areas classified as low-moderate burn severity by initial assessments. To quantify the spatio-temporal patterns and potential causes of delayed tree mortality, we combined remote sensing and field survey data for five fires burned between 1999-2003 in the western portion of GNP. We developed a remote sensing monitoring tool based on spectral and textural features derived from 1 m^2 color imagery from NAIP that produces validated time series maps of tree- to stand-level forest condition including: mature green trees, regenerating trees, dead red-phase trees, dead grey-phase trees, snags, non forest vegetation, shadows, water, and snow/ice. Based on these maps, we document that delayed tree mortality occurred throughout a substantial portion of the fires studied. Geographical variation in the magnitude and timing of delayed tree mortality was observed—in some cases delayed mortality completely transformed landscape conditions since the initial post-fire assessments, while in others it had minimal effects. Lagged detection of initial fire effects (e.g. girdling), primary and secondary bark beetles, and potentially climate all influenced the spatio-temporal patterns of delayed tree mortality that we documented. Forest cover composition was a key determinant of the likelihood of the magnitude of delayed mortality and its likely causal mechanisms. Thus, cover type may be a useful guide for prioritization of future post-fire monitoring efforts.

Introduction

Since the early 1980s, over one quarter of a million acres have burned west of the Continental Divide through forest-dominated areas of Glacier National Park (GNP). Initial aerial post-fire assessments of fire severity, a measure of tree mortality, and field observations indicate that these fires have created a mosaic of different burn severities, with substantial areas of forest surviving in moderate- and low-severity burn patches. Quantitative estimates of burn severity derived from pre- and post-fire analysis of Landsat imagery using the differenced normalized burn ratio (dNBR) for all fires > 400 ha in size within western GNP between 1984-2010 corroborate this interpretation. These data show that a minority of burn area (29%) within western GNP have burned at high severity, killing most trees, while 38% and 34% of the total burn area was influenced by low- and moderate-severity fire effects, respectively. However, field observations and aerial assessments of tree survival in previously burned areas made more recently—years after the Park's major fire events—suggest that some areas classified as low- or moderate-severity have experienced significantly higher mortality than expected based on the one year post-fire field, aerial, and remotely sensed assessments. These observations have raised the question of how much forest mortality may occur in burned areas after the one year timeframe at which most post-fire severity assessments are conducted. This question is of fundamental importance because mid- (i.e. post-fire management) to long-term (i.e. habitat management, fuels forecasting, fire modeling and suppression strategies) planning and management objectives that are based on one year post-fire assessments may not account for the changing landscape conditions that unfold following fires. If delayed post-fire mortality is

common, initial post-fire assessments may become quickly outdated in portions of the landscape. Currently, the degree, extent of and mechanisms underlying this delayed tree mortality in burned areas of GNP are not well understood.

This project addresses these knowledge gaps by (i) developing a robust remote sensing tool that uses high resolution aerial imagery to track changes in forest mortality and live vegetation structure over time, (ii) applying the tool to a network of patches within recently burned areas to estimate the magnitude and spatiotemporal patterns of delayed tree mortality caused by recent fires in western GNP, and (iii) evaluating the potential causes of delayed tree mortality using a combination of remote sensing, field data and statistical modeling.

Background

Ecological importance and causes of delayed mortality

Delayed tree mortality has been documented previously in a number of fires in different forest types within the northern U.S. Rocky Mountains (Ryan and Ammann 1994, Ryan and Ammann 1996, McHugh and Kolb 2003, Perrakis and Agee 2006, Hood et al. 2007), but it has not been systematically quantified previously. As a result, the frequency, ecological importance and causes of delayed mortality are unknown. Much of the delayed mortality observed in previous fires has been attributed to bark beetles (Ryan and Ammann 1996, Santoro et al. 2001, McHugh et al. 2003, Hood and Bentz 2007, Davis et al. 2012), whose populations may switch from endemic to epidemic levels when abundant fire-weakened host trees become susceptible to mass attack. The timing and degree of delayed mortality documented in these studies is quite variable, often occurring within 1-8 years and causing anywhere from low (5-30%) to high (60-80%) levels of post-fire tree mortality. Some of this variability is clearly contingent on the specific dynamics of unique bark beetle-host tree interactions. For instance, fires and associated increases in fire-weakened trees do not stimulate strong shifts towards epidemic outbreak stages in the mountain pine beetle (*Dendroctonus* ponderosae), the primary lethal bark beetle species affecting ponderosa and lodgepole pine (Safranyik & Wilson 2007). Rather, low level post-fire tree mortality (5-30%) in pine species has mostly been observed over short periods (1-3 years) as a result of western pine beetle (*Dendroctonus brevicomis*) or secondary bark beetles (e.g. *Ips sp.*) that tend to infest trees likely to die directly as a result of fire impacts (McHugh et al. 2003, Perrakis and Agee 2006, Davis et al. 2012). In contrast, epidemic outbreaks of Douglas-fir beetles often cause high mortality of Douglas-fir trees (30-70%) and can last for over four years following fires (Ryan and Ammann 1996, Hood and Bentz 2007). These results, however, are based on limited case studies and there is currently no robust theoretical or empirical framework that explains the great variability in the likelihood, timing and severity of post-fire bark beetle attacks that could explain delayed forest mortality in different forest cover types. Moreover, post-fire bark beetle epidemics cannot explain delayed tree mortality in a number of dominant tree species in western GNP, such as western larch or western hemlock, which do not experience lethal attack by bark beetles.

Alternative explanations of the cause of delayed mortality have not been thoroughly explored, but may include (1) climate-tree physiology-fire interactions or (2) delayed visual detection of

tree mortality due to fire. Delayed tree mortality could occur following fire as a result of interactions with pre-fire, year-of-fire, or post-fire climatic conditions that affect tree physiology and resilience. Recent research (Kavanagh et al. 2010, Michaletz et al. 2012) suggests that surface fire-induced tree death may be more due to heat impairment of xylem function, and ultimately to systemic hydraulic failure, rather than direct cambial damage. According to this hypothesis, drought in years prior to a fire may predispose trees to greater mortality independent of fire behavior simply because xylem function is already impaired when a fire occurs. Following fire, surviving trees that sustained fire-caused damage to xylem tissues may have impaired water relations and significantly reduced resilience to post-fire drought. Thus, climatic influences at multiple temporal scales may be important contributors to delayed tree mortality that warrant thorough exploration.

Finally, apparent delayed tree mortality may result from lags between fire-caused mortality and the ability to visually detect tree death. For example, surface fires may leave substantial portions of the overstory canopy intact, yet still result in widespread canopy tree mortality as a result of cambial damage, partial crown scorch, or other physiological impacts to trees. In these cases, delayed mortality does not actually occur (i.e. tree death is actually caused directly and immediately by fire) but is incorrectly inferred as a result of the delayed visual detection of tree death. This mechanism is especially likely to occur where fire-sensitive trees are present. Fire-sensitive trees often have thin bark, shallow root systems or roots that grow in duff layers (not mineral soil), and may have abundant lower crown foliage that can lead to more intense understory burning or torching (Peterson and Ryan 1986, Brown et al. 2004). In GNP, fire-sensitive species such as lodgepole pine, Engelmann spruce, subalpine fir, western red cedar, western hemlock, birch, and aspen are widespread, so there is potential for this mechanism of delayed mortality to operate within GNP. Although the mechanism of apparent delayed mortality is relatively simple in this case, the end effect is that initial fire severity assessments quickly become inaccurate as tree mortality progresses beyond what was visually apparent in the initial post-fire years.

Remote sensing methods for mapping delayed mortality

To quantify tree mortality, it is necessary to track changes either in living or dying (or both) components of stand structure for several years following fire. Existing methods for assessing fire severity (Key and Benson 2006) and mapping tree cover changes are generally not adequate for this task (Kokaly et al. 2007), principally due to their dependence on the spectral properties of medium-resolution pixel objects from sensors such as Landsat. In these images, the minimum pixel size is coarse relative to the fine-scale heterogeneity of post-fire vegetation structures in areas burned by low-moderate severity (Larson & Churchill 2012). As a result, medium-resolution sensors tend to mix the spectral properties of regenerating understory vegetation (e.g. herbaceous layers, shrubs and post-fire tree regeneration) and residual overstory layers (Lefsky et al. 2002, Wulder et al. 2012). This is problematic because understory regeneration can recover quickly after wildfire (Chen et al. 2011, Romme et al. 2016) and may dominate or saturate spectral indices of vegetation recovery (Lefsky et al. 2002) even where tree recovery or delayed overstory tree mortality continue to impact residual overstory structure. High-resolution imagery (i.e. $\leq 15m^2$ pixels) is more appropriate for the

characterization of vegetation at the tree- to stand-scale (Wulder et al. 2004a, Wulder et al. 2004b) and it has been used to characterize overstory and understory vegetation components more effectively than moderate-resolution spectral imagery (van Wagtendonk et al. 2004, Kokaly et al. 2007). Although there is a rich archive of high-resolution aerial imagery (see *Methods*) for GNP that is available from multiple sources, this resource has not been leveraged to develop methods for characterizing post-fire changes in forest structure or to evaluate the ecological ramifications of such changes.

Methods

Study areas & research design

Significant fire years in the park have occurred in 1988, 1999, 2001, and 2003, with most of the area burned occurring in 2003. Initial field visits suggested that insufficient evidence remained in areas burned in 1988, preventing accurate characterization of fire behavior, post-fire forest structures, and tree mortality agents. To account for these limitations only fire years from 1999-2003 were selected for this study. We further restricted the number of study fires by eliminating those that burned predominantly in high-severity fire regime forest zones, such as subalpine forests, where fire-sensitive species (e.g. spruce, fir) are common, trees that survive fire are rare, and delayed tree mortality is therefore unlikely to be of great ecological importance. Fires were included if they burned predominantly in cover types dominated by ponderosa pine, western larch, Douglas-fir, lodgepole pine, cedar-hemlock or mixed conifer-deciduous cover types. These selection criteria resulted in a final set of five large fires in three major fire years (Fig. 1, Table 1), including: Anaconda Fire (1999), Moose Fire (2001), Roberts Fire (2003), Harrison (2003), and Center Mountain (2003). For areas burned in these years, a time series of aerial imagery was compiled to characterize the spatial patterns of delayed tree mortality and field data were collected to evaluate the causes of delayed mortality.

Remote sensing research design and image analysis techniques

Imagery available for each of these fires years included National Agriculture Imagery Program (NAIP) imagery from 2005, 2009, 2011, and 2013, providing a 2-14 year time series of post-fire imagery. The NAIP imagery provides high resolution ($1m^2$), orthorectified, color imagery with red, green and blue bands (available for years 2005-2013) and infrared bands (available only for 2009-2013). We used this time series of imagery to (1) train and validate a predictive machine learning model of vegetation cover type and (2) use the model to map changes in vegetation cover types over the time series for a statistically valid portion of each of the five major study fires. For the first step, we manually selected 50 pixels from each of nine cover types for each year of the time series, for a total of 1,800 pixels (50 pixels/cover type * 9 cover types * 4 years). The nine cover types that we selected were: green mature trees (MT), post-fire regenerating trees (R), recently dead red-needled trees (RT), dead grey trees (GT) that have recently shed their needles, non forest vegetation comprised by shrub or herbaceous life forms (NF), long dead snags with little to no fine fuels (S), shadows (SH), snow (SN), and water (W). MT are the primary focus of this study, as they comprise trees that survived fire and are susceptible to delayed mortality. R and NF vegetation has relatively similar spectral characteristics to MT and represents the dominant understory vegetation that is most likely to cause classification errors of MT trees in post-fire environments, so it was important to assess

the ability to model overstory and understory vegetation separately. RT and GT are dead trees that are at different times since death or may capture unique species-specific spectral signatures associated with dead and dying trees. RT have died recently, likely within the last 1-3 years, whereas GT may either be recently killed trees (for species that lack a red-needle stage) or older dead trees, 3-15 years, that have shed red needles but still have fine fuels, e.g. small branch and twigs. S are trees that have been dead for longer periods of time, >10-15 years, have few fine canopy fuels remaining and are often sun-bleached. SH are widespread in forested environments and represent areas with insufficient spectral information for successful classification. SN and W are widespread features whose area may change interannually, depending on climatic conditions and the timing of imagery acquisition. Thus, it is useful to be able to mask these temporally varying features from analysis.

For each of the 1800 pixels, we extracted a series of raw and derived spectral features. Raw spectral properties included the red, green, blue and near-infrared bands. From these, we calculated two spectral ratio indices, the red-green index (RGI) and the blue-red index (BRI), calculated as:

$$\text{(Eq. 1): RGI} = \frac{DN_{Red}}{DN_{Green}} \qquad \text{(Eq. 2): BRI} = \frac{DN_{Red}}{DN_{Blue}}$$

where DN is the digital number for the subscripted bandwidth. These indices have been used in previous research (Coops et al. 2006, Meddens et al. 2011, Gartner et al. 2015, Hart and Veblen 2015) to effectively distinguish green trees and other living vegetation from dead trees in the red and grey phases. Because spectral properties alone may be insufficient to distinguish between some cover types (e.g. green overstory trees and live understory vegetation), we also calculated a series of textural features to describe the characteristic spectral variation around each pixel from the different cover type classes. Textural features can greatly improve classification results (Coops and Culvenor 2000, Franklin et al. 2000, Moskal and Jakubauskas 2013) where spectral features between cover type classes are similar. To calculate the texture features of each image, we first calculated the grey level co-occurrence matrix (GLCM) using a 5 x 5 pixel window size. This procedure (Haralick and Shanmugam 1973, Hall-Beyer 2017) calculates the number of occurrences of unique pairs of pixels in quantized grey tone levels within the specified spatial window. A series of textural indices are then calculated for the central pixel of the analysis window based on its GLCM. We used the R package *glcm* to calculate the GLCM and 8 textural indices, including: mean GLCM, GLCM variance, homogeneity, contrast, entropy, angular second moment and correlation. In total, each image pixel was associated with 14 features (4 raw spectral features, 2 derived spectral features, and 8 textural features).

Model construction

The 1,800 manually selected pixels with known cover types were split into training (70% of pixels) and validation datasets (30% of pixels) and used to build a Random Forest model using cover type as the response variable and the 14 remotely-sensed pixel features as predictors. Random Forests is a machine learning ensemble algorithm that is a robust predictor even

where high dimension, non linear relationships exist between the response and predictor variables (Breiman 2001, Cutler et al. 2007). We used the *Caret* package (Kuhn 2008) in R to tune the Random Forest parameters and to perform a 10-fold repeated cross-validation procedure to assess model performance. Repeated cross-validation is a robust method of evaluating the performance of models (Kuhn and Johnson 2013) built using the training dataset and assessed using the independent validation dataset. We repeated the cross-validation procedure 10 times to stabilize the performance measures. We used the average accuracy and Kappa statistic values from all 10 repeated cross-validations as the primary model performance measures. We used variable importance rankings to evaluate the relative importance of different spectral and textural feature predictors of cover types.

Mapping the magnitude and spatial patterns of delayed mortality

To evaluate the spatio-temporal patterns of delayed mortality across the five study fires, we applied the Random Forest model predict changes in cover types for a subset of spatially distributed patches in each of the five fires that experienced low-moderate fire severity. We used dNBR maps (Key & Benson 2006) from the Monitoring Trends in Burn Severity program to exclude burn areas that were influenced by high severity fire. Areas affected by high severity were excluded because these areas had little tree survival and therefore could not experience substantial delayed mortality. We then used the GNP vegetation layer, derived from visual photointerpretation of color infrared imagery from the late 1990s (prior to our study fires) as the basis for selecting patches from the remaining portions of each fire in this study. The GNP vegetation layer groups areas with similar species composition and structural features (e.g. canopy cover), making them an appropriate unit for comparison of the ecological response to fire and patterns of delayed mortality between unique forest types. Patch forest types in our study fires from the GNP vegetation data layer include: western larch, Douglas-fir, ponderosa pine woodland, lodgepole pine, cedar-hemlock, and spruce-fir. We selected 40 spatially distributed patches within each of the five fires and in all forest types and we modeled changes in cover types within each study patch over the 2005-2013 period. Based on the observed cover type changes, delayed mortality was calculated as the percent of all non-shadowed pixels (e.g. the percent of patch area with spectral information) consisting of green mature trees between each time interval (e.g. 2005 to 2009) and for the overall period (2005-2013). To identify trends in other cover types and evaluate the utility of our model data products for tracking ecological change, fuel structures and habitat characteristics, we also explored changes in other cover types over time.

Causes of delayed mortality

We evaluated climate at 3 time steps (pre-fire, year-of-fire, and one to five years post-fire) and beetle outbreaks as the principal potential causes of delayed mortality other than delayed visual detection.

We used observed monthly climate data from Division 1 (northwestern MT) of the National Climate Data Center (NOAA) to examine climatic conditions that might influence delayed mortality for the fire years studied. We used the Palmer's Drought Severity Index, calculated for the April-September months for each year, to represent regional drought severity because the

PDSI is an integrated measure of temperature and precipitation that is closely linked to plant physiology (Stephenson 1990). To represent both the average condition and capture short (i.e. individual months) but extreme drought events, we determined the mean and minimum growing season PDSI values for each of the three time steps for each fire year. In addition to the one year post-fire drought calculations, we also calculated post-fire drought indices over a five year period to account for longer term chronic drought periods.

To determine the extent and degree of beetle outbreak following fires, we conducted detailed field surveys in 2015 in a subset of the patches where delayed mortality was assessed via remote sensing. The purpose of these field surveys was to quantify species-specific tree mortality patterns, to document the presence of bark beetle species and measure the degree of beetle-caused mortality, to measure fire effects and fire behavior, and to document post-fire forest structures. Field plots were relatively evenly distributed between fire events and across all of the forest cover types found in our study fires. In order to validate our remote sensing interpretations over the full range of forest conditions, to have a set of control plots that were unaffected by fire (and potentially delayed mortality), and to evaluate the degree and causes of tree mortality in unburned stands, we also sampled plots in set of unburned patches. We sampled 2-4 plots per sample patch, spaced along a 420m randomly-generated sample grid, to ensure that a representative sample was collected from each patch. Each plot consisted of a 15m radius circular area placed around the random grid point. From all trees above 4 cm DBH in each plot, we collected the following information: diameter at breast height (DBH), species, tree status (live or dead), tree canopy position (suppressed, intermediate, dominant, or emergent), beetle species presence as determined by examination of sub-cortical larval galleries and entrance/exit holes, the average percent of the bole affected by beetle galleries between ground level and DBH, the mortality agent for dead trees, the maximum char height and the maximum percent of the bole circumference that was charred. We surveyed trees for both primary (lethal) and secondary (generally non lethal) beetle species that could affect any of the major tree species in our study area (Table 2). The mortality agent and timing of death were determined based on the condition of each tree and evidence of bark beetle attack (Table 3). If a tree showed evidence of attack by primary bark beetles, we assigned bark beetles as the cause of mortality. If only secondary bark beetle species were present or no evidence of any beetle attack was found, we assumed that fire or an unknown factor (e.g. climate, pathogens) was the ultimate cause of tree mortality.

We calculate the plot-scale beetle attack severity as the percent of the plot basal area of trees killed by primary and secondary bark beetles relative to the total number of trees alive following the fire. To evaluate tree species-specific rates of mortality due bark beetles, we calculate the percentage of each tree species killed by primary and secondary beetles.

Because most of the burn area in western GNP examined in this study were from two fire seasons, the 2001 and 2003 fire years, a robust statistical analysis of the causes of delayed mortality was not possible. Instead, we examine climate and field data to provide the most likely explanation for the patterns of observed delayed mortality.

Results

Remote sensing of cover class features and model performance

Spectral characteristics of the nine cover types were similar between images taken in the same acquisition year (data not shown) and although they were generally similar for each cover type between acquisition years, some marginal spectral differences between cover types were apparent (Fig. 2). When grouping pixels from all years together, clear differences in the spectral (Fig. 3) and textural (Fig. 4) features of each cover type were apparent. The spectral characteristics of green mature tree were most similar to regenerating trees, but were distinguishable using multiple texture features. The Random Forest models of cover types showed relatively high performance (Table 4a, Accuracy= 72-90%, Kappa=0.7-0.89). Model performance varied when constructed for each year individually, but an aggregate model built from all years performed as well as two of the individual year models. Based on these results, we used the aggregate model from all years for cover type modeling. The accuracy of specific cover type classes varied between models for different years, but some consistent trends were apparent (Table 4a). Red trees, grey trees, snags, non forest, shadows, snow, and water all had consistently high accuracies (mostly above 85%). Green mature and regenerating trees had more variable and slightly lower accuracies (mostly > 75%). Comparison of predicted vs. actual cover type (Table 4b) show a number of notable patterns. The models generally over-predicted the cover of mature green trees, mostly due to misclassification errors between mature and regenerating trees. Misclassifications between red and grey trees accounted for the majority of errors in these cover types, although grey trees were also occasionally misclassified as snags or green trees. Non forest was most frequently misclassified as regenerating forest.

Figure 6 shows the modeled cover types for an entire patch and for a closeup section of the same patch over the period 2005-2013. Similar patterns of delayed mortality are evident in comparisons of the aerial photographs and the modeled cover type maps. This patch was heavily forested, with high canopy cover of green trees, immediately following the fire. By 2005, significant tree mortality (red- and grey-stage trees) and some type conversion to non forest was apparent. Red trees had disappeared from the patch by 2009 and it was dominated by a mixture of mature green canopy cover at levels similar to those in 2005 and grey trees. By 2011, a notable proportion of the patch was in a non forest state and the cover of red trees increased again, although not to the same levels as 2005. Similar canopy cover values in 2009 and 2011, despite the increase in non forest area, may be in part a result of the higher number of shaded pixels in 2005 and 2009 compared with 2011. By 2013, non forest area had expanded and was reflected in a marked decrease in canopy cover. Few red trees were present in 2013, suggesting that continued mortality in this patch had stabilized. Patterns in this patch are not necessarily reflective of the larger patterns within GNP. We present them here to demonstrate the approach used to quantify delayed mortality across all patches in the study area, to illustrate the key patterns that can be detected with the remote sensing and machine learning modeling approach developed here, and to highlight the dramatic changes caused by delayed mortality in some portions of GNP.

Landscape patterns of delayed mortality

The degree and distribution of delayed tree mortality in GNP was highly variable and likely driven by multiple factors. From 2005-2013, there was a trend towards decreasing canopy cover across the western portion of the park that was strongest between 2005 and 2011. On average, the median canopy cover of patches affected by wildfire declined from 74% in 2005 to 62% in 2011, which represents a significant but not dramatic effect of delayed mortality overall. However, there was substantial variation around the average trends (Fig. 7) that is evidence of dramatic declines in canopy cover due to delayed mortality in portions of the park, even in areas that experienced very low tree mortality directly by fire (e.g. Fig. 6). Some of the variability in the degree of delayed mortality is related to the dominant species composition of different patches. While delayed mortality was observed in all forest types to some degree (Fig. 7b-g), certain forest types were more susceptible to delayed mortality than others. In particular, ponderosa pine, Douglas-fir, and lodgepole pine forest types experienced notable delayed mortality, whereas western larch, spruce-fir and cedar-hemlock stands had mild or no no trends at all. Interestingly, a trend that was apparent in western GNP overall and several individual forest types, in particular, was a slight increase in canopy cover between the 2011-2013 period. This could be partially due to radiometric differences in the imagery acquired between years that affected model performance between years or it could reflect a real ecological trend. Ecologically, this trend could be explained by recovery of leaf area by fire-affected trees, especially those that were heavily scorched by fire, canopy expansion in surviving trees due to reduced competition to light, or epicormic sprouting (Hanson and North 2006). Significant post-fire recovery of trees heavily damaged by fire have been observed in field studies of similar forest types in the region (Leirfallom and Keane 2011) and both western larch and Douglas-fir have the potential for epicormic sprouting following fire (Schmidt et al. 1976, Bryan and Lanner 1981). Both of these explanations are consistent with the much stronger positive trends in canopy cover over the 2011-2013 period in ponderosa pine-Douglas fir and western larch patches (Fig. 7b, d) compared to other cover types.

The declines in canopy cover that were observed in burned stands were not apparent over the same time period in adjacent unburned patches (Fig. 8). In unburned patches, canopy cover remained relatively constant, with only small variations, and this effect was consistent across all vegetation types. These patterns both confirm the quality of our remote sensing approach and highlight that delayed mortality is a cascading ecological process triggered by fire. Some of the variation evident in these stands may represent low levels of bark beetle-caused mortality, other pathogenic or climate-driven marginal losses in canopy cover, or relictual effects of our analysis that resulted from image quality differences between years (i.e. the extent of shadows) or model errors.

The magnitude and timing of delayed mortality varied between the five fires studied (Fig. 9). Interestingly, delayed mortality was detected in the 1999 Anaconda and 2001 Moose Fires, although to a lesser degree than in most of the 2003 fires, during 2009 and 2011, indicating that delayed mortality can occur for over 10 years after fire. The most severe delayed mortality occurred in the Center Mountain and Harrison Fires during 2011-13, resulting in decreases from median live tree canopy cover values of ~60% to < 40%.

Field plot observations of mortality agents

In total, we surveyed 84 burned plots, primarily in patches burned by low severity fire, and 34 unburned plots. In total, we determined the condition and causes of mortality in 7,490 trees (Table 1, Table 5, Table 6). Of the 84 burned plots, surveys in 51 plots ("Full" plots) included full surveys of post-fire forest structure, tree condition and mortality agents while 33 plots ("Structure" plots) only included surveys of post-fire forest structure. Most unburned plots showed very low levels of beetle attack, mostly by primary bark beetle species that affected < 10% of plot basal area (Table 5). Many burned plots, on the other hand, showed no evidence of beetle attack. However, those that did generally experienced much higher beetle attack severity (up to 35% of plot basal area). The percentage of plots attacked and the severity of post-fire bark beetle attack varied by forest cover composition. Primary bark beetle attack was most severe in ponderosa pine, Douglas-fir and spruce-fir forest types and was lowest for lodgepole pine and cedar-hemlock forests. Secondary beetles (mostly *Ips pini*, *Pseudohylesinus nebulosus,* and *Scolytus unispinosus*) were most abundant in ponderosa pine, Douglas-fir and lodgepole pine forests. Most trees in burned plots were killed by fire (32-94%) and few (< 1%) had been killed by bark beetles prior to fire (Table 6). The most severe post-fire tree mortality caused by primary beetles was observed for Douglas-fir (29%) and Engelmann spruce (58%) trees and was caused by the Douglas-fir (*Dendroctonus pseudotsugae*) and spruce (*Dendroctonus rufipennis*) bark beetles. Post-fire secondary bark beetle attacks were most severe for true firs (63-79%), pine species (26%-41%), and Douglas-fir (20%).

Causes of delayed mortality

Although the largest fire year in GNP, the 2003 fire year, was characterized by a period of significant drought, both the 2001 and 1999 fire years had more significant drought events either preceding or following them (Table 7a). For the 1999-2001 fires, our time series from 2005-2013 begins 4-6 years post-fire, a time when delayed mortality may be at its highest. Unfortunately, we cannot quantify delayed mortality in the 1999 and 2001 fires during these critical years using our time series and we cannot therefore directly evaluate the influences of pre- and post-fire climate on delayed mortality in these fires.

For the 2003 fires, the most dramatic declines in canopy cover resulting from delayed mortality in our time series occurred during 2011 or 2013, depending on the fire (Fig. c-e). This represents a range of 8-10 years post-fire over which delayed mortality peaked. Climate data show that atmospheric water deficit during the year preceding the 2003 fire and for five years post-fire (Table 7a) was generally quite low. The most significant drought events following 2003 were in 2007 and to a lesser extent in 2009. Therefore, the years of peak delayed mortality for the 2003 fires do not coincide directly with climatic conditions that would augment physiological tree mortality due to water stress. However, lagged effects (Bigler et al 2007), such as bark beetle attack, can be triggered by drought, leading to widespread tree mortality several years after a drought event (Chapman et al. 2012).

Although we do not quantify delayed mortality in years 1-2 post-fire for the 2003 fire, visual comparisons of the 2003 burn area in fall of 2003, after the fire had subsided, with the 2005 NAIP imagery shows that significant loss of green canopy cover had already occurred in some

areas by 2005 (Figs. 1, 6). This pattern of significant delayed mortality most apparent in the Middle Fork Complex fires (Center Mountain and Harrison Fires) and southwestern portions of the Robert fire, where forests were heavily dominated by even-aged lodgepole pine forests regenerating mostly after 2 major fire years in 1910 and 1929 (Barrett 1986, Naficy 2017). Not only were climatic conditions relatively mild following the 2003 fires, but we also observed very low levels of primary beetle attack in lodgepole pine trees within these forests. The most likely explanation of the extensive delayed mortality in these stands that was apparent in 2005 is that relatively low intensity surface fire behavior in 2003 left tree canopies largely intact and led to the classification of these stands in the dNBR analysis as low severity. However, fire intensity appears to have been sufficient to effectively girdle these thin-barked, fire-sensitive trees and result in tree mortality that began immediately following the fire and was fairly widespread already in 2005. We also documented very high levels of secondary beetle attack by *Ips pini* in many lodgepole pine trees in the Roberts, Center Mountain and Harrison fires that may have compounded tree mortality in initial or subsequent years. For the 2003 fires, it appears that two pulses of delayed mortality occurred, one immediately following the fire during 2004-2005 and another during the 2011-2013 period. It is likely that the first pulse of delayed mortatliy was at least partially caused by tree girdling effects of the fire directly, although secondary bark beetles may also have contributed to this event. However, during the second pulse of delayed mortality that occurred 8-10 years post-fire, girdling is an unlikely explanation. It is possible that drought conditions in 2007 or 2009 contributed to outbreaks of *Ips pini* that caused the second wave of delayed mortality observed in our remote sensing analysis. Unfortunately, because no samples from beetle-infested trees were collected in our field samples, we cannot address the timing of secondary bark beetles.

Compared to these patterns in lodgepole pine-dominated forest, delayed mortality was most apparent in Douglas-fir and mixed-conifer ponderosa pine/Douglas-fir cover types. The cause of much of this mortality was clearly a result of widespread, moderate-severity tree mortality by the Douglas-fir bark beetle. This is consistent with field surveys of Douglas-fir beetle mortality in the Moose fire of 2001 (Hood & Bentz 2007), which showed ongoing moderate-severity beetle attack (~ 60% of stand density) in Douglas-fir trees for up to four years. Whereas the attacks by *Ips pini* in lodgepole pine were spatially biased towards the southern portion of GNP, the Douglas-fir bark beetle was observed in stands with susceptible hosts throughout GNP. The western pine beetle caused high ponderosa pine mortality in some stands but its distribution was very patchy.

Discussion

The diverse patterns and causes of delayed mortality that we document here highlight the cascading processes that can be triggered by fire. Delayed mortality significantly altered landscape-scale vegetation conditions in GNP after initial assessments based on dNBR were made, although there was significant geographic variability in these patterns. Although we could not effectively address the role that climate-induced tree stress may play in driving delayed mortality, we have documented the strong influence of tree species composition on the potential trends that could be expected following fire. Stands of western larch, and cedar-hemlock forest, were much less likely to experience delayed mortality than ponderosa pine,

Douglas-fir or lodgepole pine. Not only does the susceptibility of delayed mortality depend on forest composition, but so does the mechanism. In ponderosa pine/Douglas-fir and pure Douglas-fir stands, primary bark beetles were a major source of delayed mortality. However, in lodgepole pine stands primary bark beetles were rarely present and caused little of the observed delayed mortality. Rather, delayed mortality was likely a result of fire effects that either girdled trees at the time of fire or made them susceptible to attack by secondary beetles or other external mortality agents.

We show that delayed mortality is an ecologically important process in GNP. If projected climate-driven increases in wildfire frequency and area burned are realized(Barbero et al. 2015), it ~~that~~ can be expected to continue to shape the landscape of GNP. A striking finding of this research is that the process of delayed mortality can occur for many years following fire, up to almost a decade. This highlights that post-fire environments are highly dynamic and that post-fire monitoring of landscape condition is necessary beyond the one-year initial assessments that are most common. Since this study began, GNP has experienced multiple significant fire years. The high variability in the timing and geographic patterns of delayed mortality require a tool that can be used to understand evolving landscape vegetation conditions and patterns. We have developed a remote sensing work flow and modeling framework that can be built upon to monitor fire-caused tree mortality and residual forest structural characteristics using the widely available and recurrent imagery acquisitions through NAIP. The tool can be updated to incorporate imagery from new years to continue tracking landscape conditions in both old and new fires. Thus, this tool offers a cost-effective monitoring tool that is well-suited to produce high quality maps for a suite of applications, including: fuel mapping, wildlife habitat maps, post-fire recovery rates, bark beetle outbreaks in unburned forests, and detection of climate-induced forest dieback.

Limitations

There are some limitation to our approach. Key among these are limitations that arise from the NAIP imagery products themselves. NAIP imagery is provided as an orthorectified product with georegistration errors of several pixels or approximately 5-10 m (NAIP 2017), depending on the imagery provider for each year. This degree of geographic error makes it difficult to track individual image objects (i.e. trees) across the time series as part of an automated workflow. For this reason, we used patches that are many times larger than the NAIP georegistration errors as our fundamental study units. The small georegistration errors, relative to the patch sizes used, is unlikely to have biased cover type distributions for each time step. However, higher quality semi-automated orthorectification is possible for a landscape the size of GNP and would allow much improved temporal tracking of specific features in the landscape.

Our model tended to overpredict green canopy vegetation and had the highest error rates for distinguishing between mature green and regenerating green trees. The incorporation of image texture into the classification procedure was critical to the Random Forest models ability to distinguish between these, and other, features that are difficult to separate based only on spectral features (Fig. 5). However, textural features are scale-dependent indices (Hall-Beyer 2017) and can be incorporated into pixel-based (as done here) or object-based classification

systems (Moskal & Jakubauskas 2013). Future work to address scale impacts on texture indices or incorporate them into object-based classification procedures are warranted and could improve our results significantly.

Conclusions

Fires create abrupt change in landscape conditions and functions that can be measured in initial post-fire assessments (Key & Benson 2006). However, it also initiates cascading ecological processes and change that may not be linearly related to initial post-fire conditions and therefore require consistent monitoring. To address this need, we developed a remote sensing monitoring tool based on 1 m^2 color imagery from NAIP that produces time series maps of tree- to stand-level forest condition and cover type based on spectral and textural pixel features. Because NAIP is a federal program that is consistently updated every 3-4 years, our toolset could be expanded to include other portions of GNP and used as a regular monitoring and inventory tool of landscape condition within GNP.

In this study, we used the remote sensing toolset to document that delayed post-fire tree mortality is an important cascading process that shapes burned areas for up to almost a decade following fire. We found strong geographic variability in the magnitude and timing of delayed mortality—in some cases delayed mortality completely transformed landscape conditions since the initial post-fire assessments, while in others it had minimal effects. Lagged detection of initial fire effects (e.g. girdling), primary and secondary bark beetles, and potentially climate all influenced the spatio-temporal patterns of delayed tree mortality that we documented. Forest cover composition was a key determinant of the likelihood of delayed mortality and its likely causal mechanisms. Thus, cover type may be a useful guide for prioritization of future post-fire monitoring efforts.

Acknowledgements

We thank Dennis Divoky, Dave Soleim, Tara Carolin, and Kris Peterson, without whom this project would not have been successfully undertaken. For assistance with field work, we thank Drew Carter and Jessica Jenne.

Bibliography

Barbero, R., J. T. Abatzoglou, N. K. Larkin, C. A. Kolden, and B. Stocks. 2015. Climate change presents increased potential for very large fires in the contiguous United States. International Journal of Wildland Fire:-.

Barrett, S. W. 1986. Fire History of Glacier National Park; Middle Fork Flathead River Drainage. National Forest Service.

Breiman, L. 2001. Random forests. Machine Learning **45**.

Brown, R. T., J. K. Agee, and J. F. Franklin. 2004. Forest restoration and fire: Principles in the context of place. Conservation Biology **18**:903-912.

Bryan, J. A. and R. M. Lanner. 1981. Epicormic branching in Rocky Mountain Douglas-fir. Canadian Journal of Forest Research **11**:190-200.

Chen, X. X., J. E. Vogelmann, M. Rollins, D. Ohlen, C. H. Key, L. M. Yang, C. Q. Huang, and H. Shi. 2011. Detecting post-fire burn severity and vegetation recovery using multitemporal remote sensing spectral indices and field-collected composite burn index data in a ponderosa pine forest. International Journal of Remote Sensing **32**:7905-7927.

Coops, N. and D. Culvenor. 2000. Utilizing local variance of simulated high spatial resolution imagery to predict spatial pattern of forest stands. Remote Sensing of Environment **71**:248-260.

Coops, N. C., M. Johnson, M. A. Wulder, and J. C. White. 2006. Assessment of QuickBird high spatial resolution imagery to detect red attack damage due to mountain pine beetle infestation. Remote Sensing of Environment **103**:67-80.

Cutler, D. R., T. C. Edwards, K. H. Beard, A. Cutler, and K. T. Hess. 2007. Random forests for classification in ecology. Ecology **88**:2783-2792.

Davis, R. S., S. Hood, and B. J. Bentz. 2012. Fire-injured ponderosa pine provide a pulsed resource for bark beetles. Canadian Journal of Forest Research **42**:2022-2036.

Franklin, S. E., R. J. Hall, L. M. Moskal, A. J. Maudie, and M. B. Lavigne. 2000. Incorporating texture into classification of forest species composition from airborne multispectral images. International Journal of Remote Sensing **21**:61-79.

Gartner, M. H., T. T. Veblen, S. Leyk, and C. A. Wessman. 2015. Detection of mountain pine beetle-killed ponderosa pine in a heterogeneous landscape using high-resolution aerial imagery. International Journal of Remote Sensing **36**:5353-5372.

Hall-Beyer, M. 2017. Practical guidelines for choosing GLCM textures to use in landscape classification tasks over a range of moderate spatial scales. International Journal of Remote Sensing **38**:1312-1338.

Hanson, C. T. and M. P. North. 2006. Post-fire epicormic branching in Sierra Nevada Abies concolor (white fir). International Journal of Wildland Fire **15**:31-35.

Haralick, R. M. and K. Shanmugam. 1973. Textural features for image classification. IEEE Transactions on systems, man, and cybernetics:610-621.

Hart, S. J. and T. T. Veblen. 2015. Detection of spruce beetle-induced tree mortality using high- and medium-resolution remotely sensed imagery. Remote Sensing of Environment **168**:134-145.

Hood, S. and B. Bentz. 2007. Predicting postfire Douglas-fir beetle attacks and tree mortality in the northern Rocky Mountains. Canadian Journal of Forest Research **37**:1058-1069.

Hood, S., B. Bentz, K. Gibson, K. C. Ryan, and G. DeNitto. 2007. Assessing Post-fire Douglas-fir Mortality and Douglas-fir Beetle Attacks in the Northern Rocky Mountains. RMRS GTR-199:31.

Kavanagh, K., M. B. Dickinson, and A. S. Bova. 2010. A Way Forward for Fire-Caused Tree Mortality Prediction: Modeling a Physiological Consequence of Fire. Fire Ecology **6**:80-94.

Key, C. H. and N. C. Benson. 2006. Landscape Assessment: Sampling and Analysis Methods. RMRS-GTR-164-CD, U.S. Department of Agriculture, Forest Service, Rocky Mountain Research Station, Fort Collins, CO.

Kokaly, R. F., B. W. Rockwell, S. L. Haire, and T. V. V. King. 2007. Characterization of post-fire surface cover, soils, and burn severity at the Cerro Grande Fire, New Mexico, using hyperspectral and multispectral remote sensing. Remote Sensing of Environment **106**:305-325.

Kuhn, M. 2008. Building predictive models in R using the caret package. Journal of Statistical Software **28**:1-26.

Kuhn, M. and K. Johnson. 2013. Applied predictive modeling. Springer-Verlag, New York.

Lefsky, M. A., W. B. Cohen, G. G. Parker, and D. J. Harding. 2002. Lidar remote sensing for ecosystem studies. Bioscience **52**:19-30.

Leirfallom, S. B. and R. E. Keane. 2011. Six-year post-fire mortality and health of relict ponderosa pines in the Bob Marshall Wilderness Area, Montana. USDA Forest Service, Rocky Mountain Research Station, Fort Collins, Colorado, USA.

McHugh, C. W. and T. E. Kolb. 2003. Ponderosa pine mortality following fire in northern Arizona. International Journal of Wildland Fire **12**:7-22.

McHugh, C. W., T. E. Kolb, and J. L. Wilson. 2003. Bark beetle attacks on ponderosa pine following fire in Northern Arizona. Environmental Entomology **32**:510-522.

Meddens, A. J. H., J. A. Hicke, and L. A. Vierling. 2011. Evaluating the potential of multispectral imagery to map multiple stages of tree mortality. Remote Sensing of Environment **115**:1632-1642.

Michaletz, S. T., E. A. Johnson, and M. T. Tyree. 2012. Moving beyond the cambium necrosis hypothesis of post-fire tree mortality: cavitation and deformation of xylem in forest fires. New Phytologist **194**:254-263.

Moskal, L. and M. Jakubauskas. 2013. Monitoring Post Disturbance Forest Regeneration with Hierarchical Object-Based Image Analysis. Forests **4**:808.

Naficy, C. E. 2017. A cross-scale assessment of historical fire severity patterns, landscape dynamics, and methodological challenges in mixed-severity fire regimes of the northern U.S. Rockies. University of Colorado, Boulder, CO.

Perrakis, D. D. B. and J. K. Agee. 2006. Seasonal fire effects on mixed-conifer forest structure and ponderosa pine resin properties. Canadian Journal of Forest Research **36**:238-254.

Peterson, D. L. and K. C. Ryan. 1986. Modeling postfire conifer mortality for long-range planning. Environmental Management **10**:797-808.

Romme, W. H., T. G. Whitby, D. B. Tinker, and M. G. Turner. 2016. Deterministic and stochastic processes lead to divergence in plant communities 25 years after the 1988 Yellowstone fires. Ecological Monographs **86**:327-351.

Ryan, K. C. and G. Ammann. 1996. Bark beetle activity and delayed tree mortality in the Greater Yellowstone area following the 1988
fires. Pages 151-158 *in* Ecological implications of fire in Greater Yellowstone Proceedings. International Association WIldliand Fire, Fairland, WA.

Ryan, K. C. and G. D. Ammann. 1994. Interactions Between Fire-Injured Trees and Insects in the Greater Yellowstone Area.*in* Plants and Their Environments: Proceedings of the First Biennial Scientific Conference on the Greater Yellowstone Ecosystem, Mammoth Hot Springs Hotel, WY.

Santoro, A. E., M. J. Lombardero, M. P. Ayres, and J. J. Ruel. 2001. Interactions between fire and bark beetles in an old growth pine forest. Forest Ecology and Management **144**:245-254.

Schmidt, W. C., R. C. Shearer, and A. L. Roe. 1976. Ecology and silviculture of western larch forests. US Department of Agriculture, Forest Service.

Stephenson, N. L. 1990. Climatic Control of Vegetation Distribution - the Role of the Water-Balance. American Naturalist **135**:649-670.

van Wagtendonk, J. W., R. R. Root, and C. H. Key. 2004. Comparison of AVIRIS and Landsat ETM+ detection capabilities for burn severity. Remote Sensing of Environment **92**:397-408.

Wulder, M. A., R. J. Hall, N. C. Coops, and S. E. Franklin. 2004a. High spatial resolution remotely sensed data for ecosystem characterization. Bioscience **54**:511-521.

Wulder, M. A., J. C. White, S. Coggins, S. M. Ortlepp, N. C. Coops, J. Heath, and B. Mora. 2012. Digital high spatial resolution aerial imagery to support forest health monitoring: the mountain pine beetle context. Journal of Applied Remote Sensing **6**.

Wulder, M. A., J. C. White, K. O. Niemann, and T. Nelson. 2004b. Comparison of airborne and satellite high spatial resolution data for the identification of individual trees with local maxima filtering. International Journal of Remote Sensing **25**:2225-2232.

Figure 1. Figure depicting the study area, remote sensing and field sampling design (upper panels) and an example of the patterns of delayed mortality in the Center Mountain-Harrison fires of 2003 over the 2003-2013 period. The upper panel shows the perimeters for fires examined in this research (red polygons), patches where delayed mortality was mapped using the time series of aerial photographs (dark grey polygons), and field plots (black triangles) where the causes of tree mortality were assessed. The closeup of a portion of the Center Mountain-Harrison fires of 2003 in the lower panels shows the spatial patterns of burn severity derived from dNBR analysis, a color aerial image taken immediately after the fire in September of 2003, and color images from the NAIP program for 2005, 2009, 2011 and 2013. The scale bar is the same for all images in the time series.

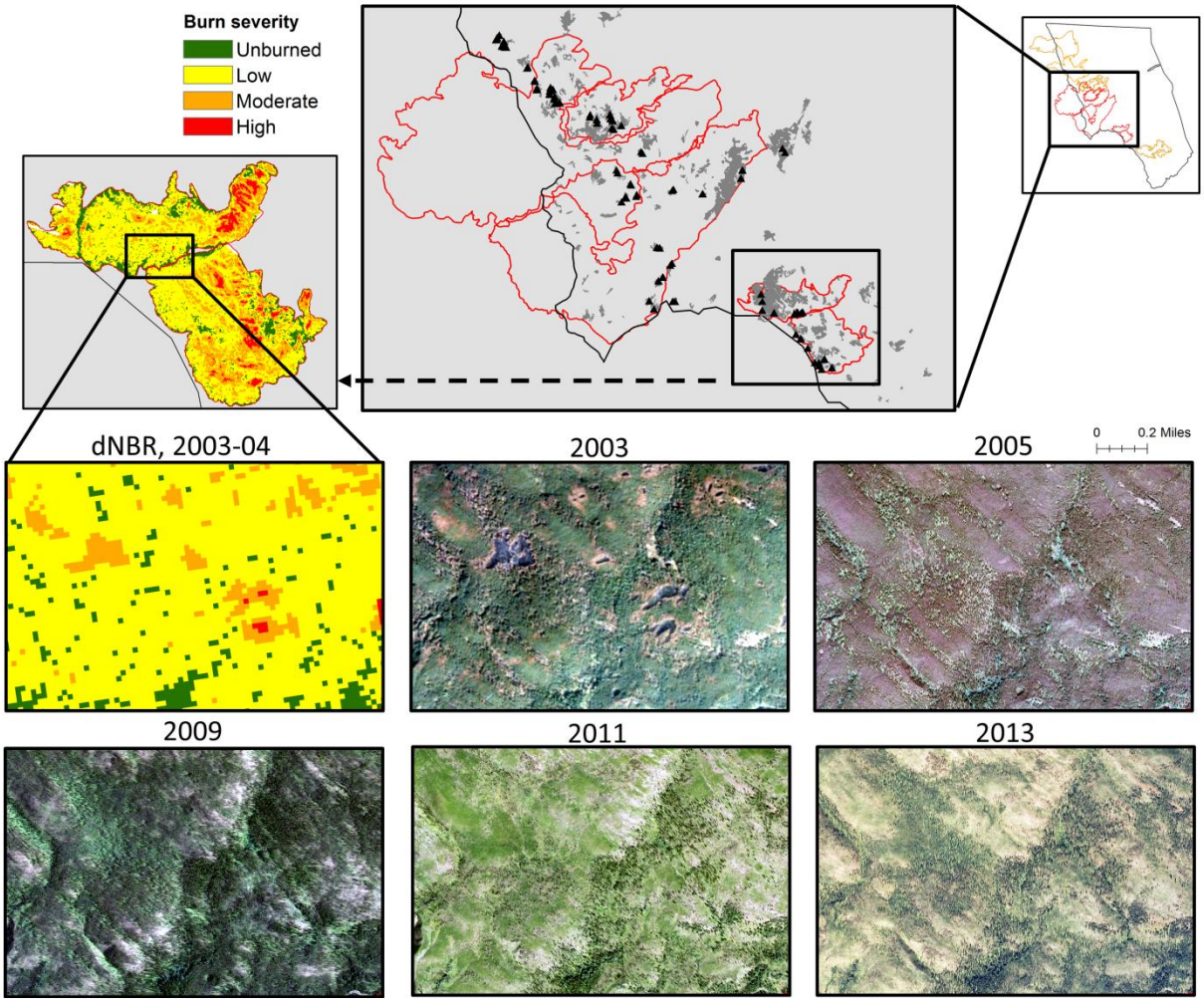

Figure 2. Summary of the spectral characteristics of cover types grouped by year of imagery. Note that 2005 imagery did not include measurements in the NIR.

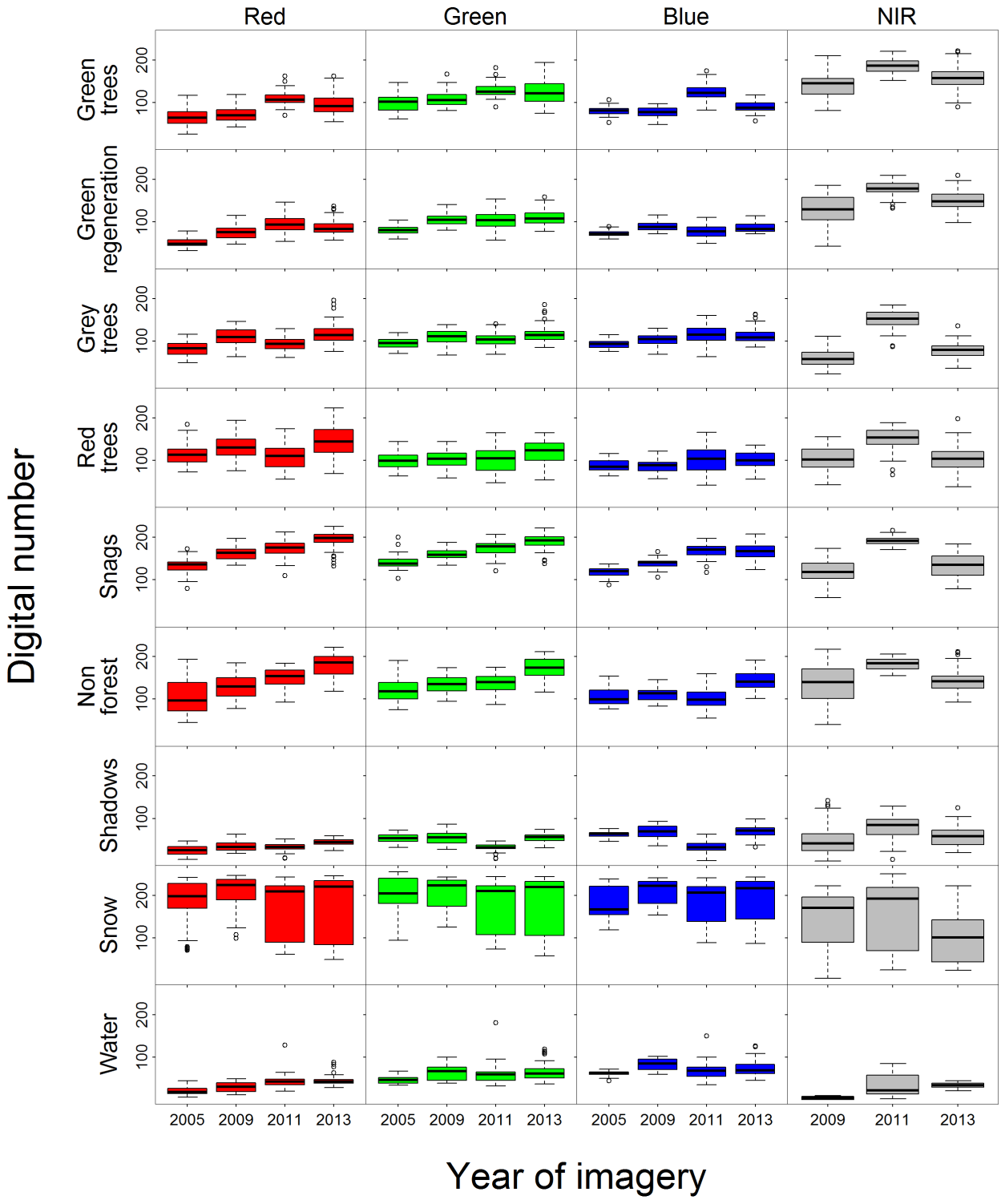

a)

Figure 3. Summary of the spectral characteristics of all cover types aggregated across years: a) red band, b) green band, c) blue band, d) near infrared, e) red-green index, f) blue-red index. Cover types are abbreviated as: MT=mature green trees, R=regenerating post-fire green trees, GT=grey trees, RT=red trees, S=snags, NF=non forest, SH=shadows, SN=snow, and W=water.

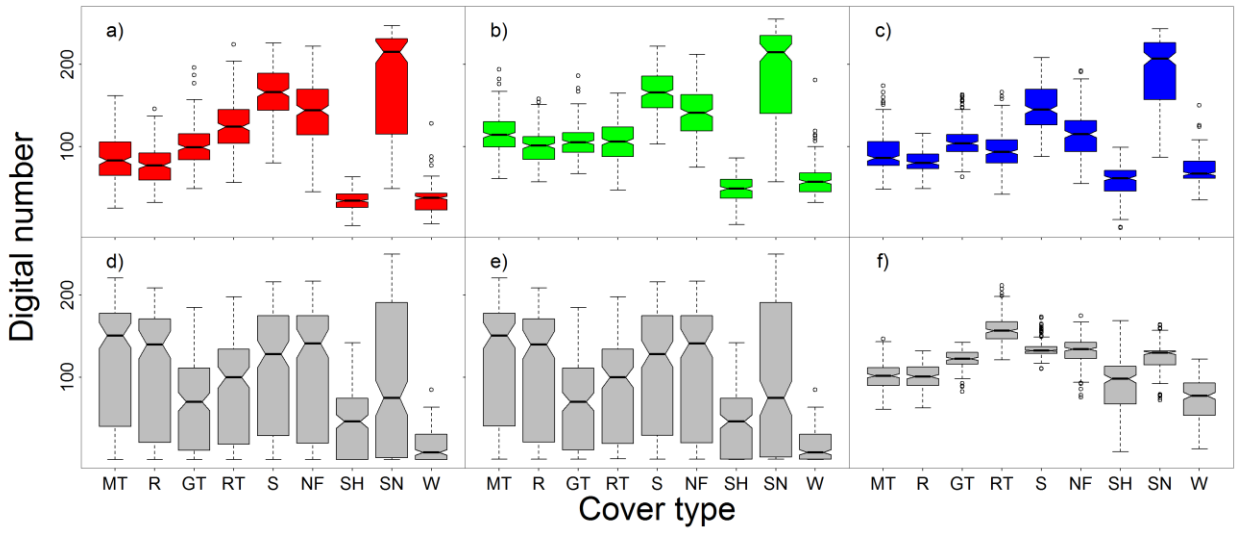

Figure 4. Summary of the textural characteristics calculated from the grey level co-occurrence matrices (GLCMs) using a 5-pixel kernel for all cover types aggregated across years: a) mean GLCM, b) GLCM entropy, c) GLCM variance, d) GLCM homogeneity, e) GLCM angular second moment, f) GLCM correlation, g) GLCM dissimilarity, and h) GLCM contrast. Cover types are abbreviated as: MT=mature green trees, R=regenerating post-fire green trees, GT=grey trees, RT=red trees, S=snags, NF=non forest, SH=shadows, SN=snow, and W=water.

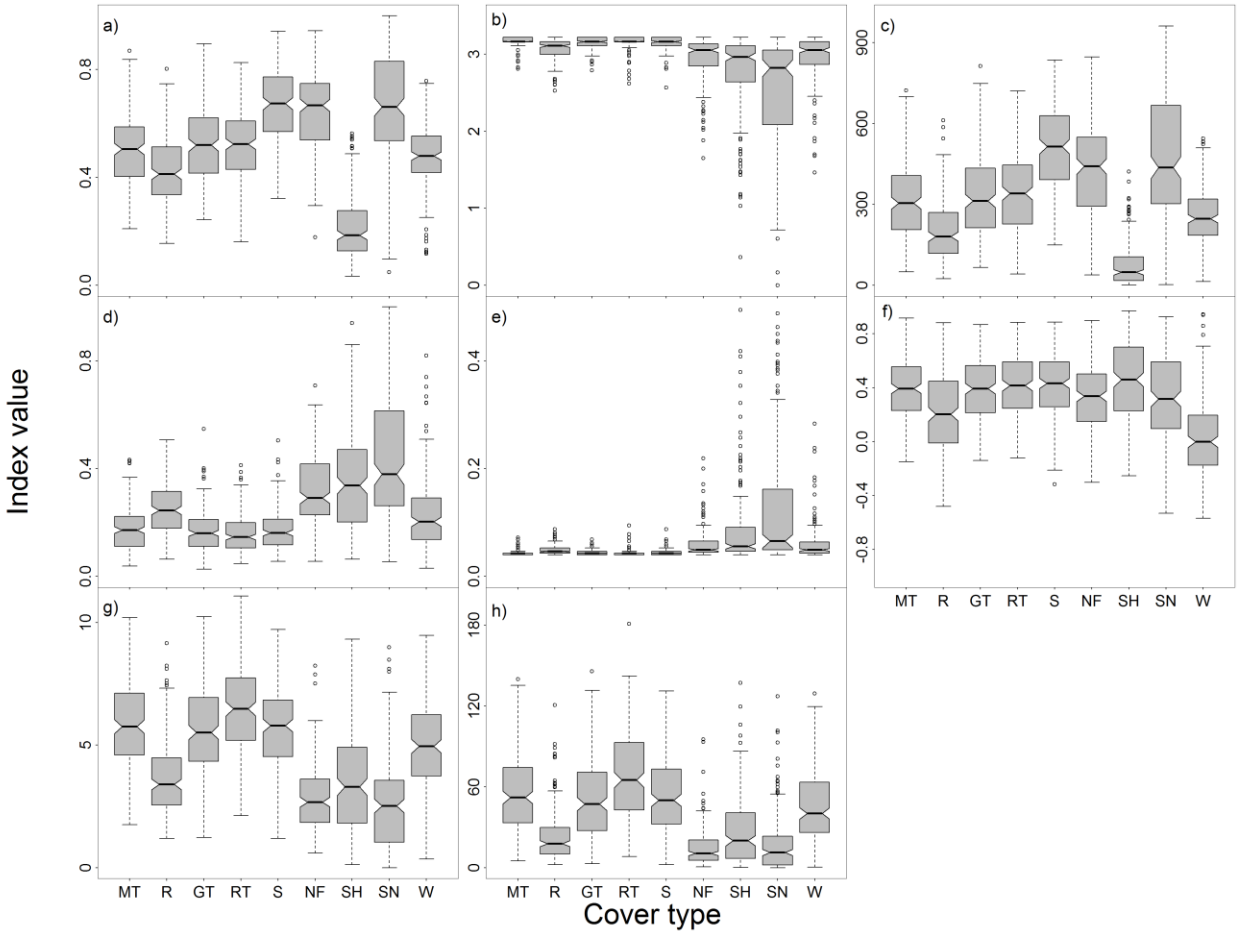

Figure 5. Example classification tree showing the relationships between the 14 remotely sensed predictors and the classified pixel cover type.

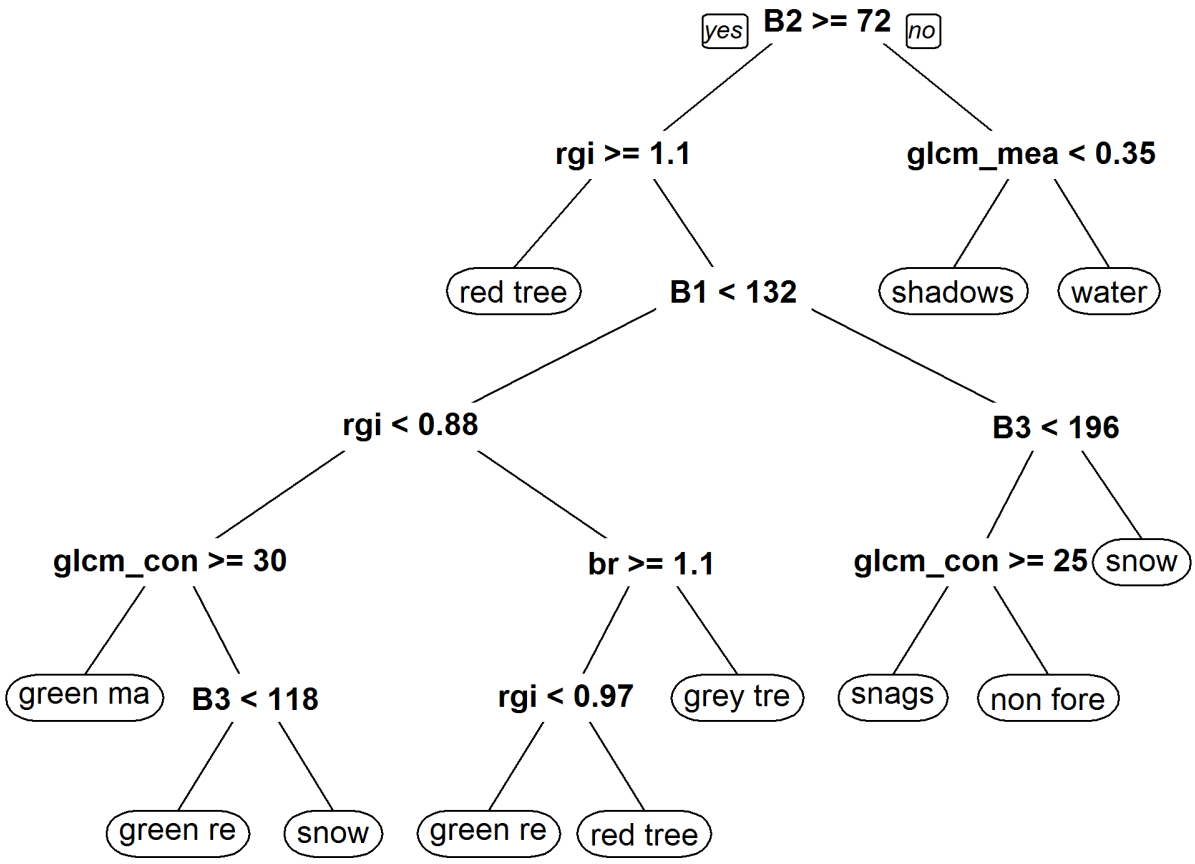

Figure 6. Images of an example patch from the 2003 Harrison Fire where cover types were modeled from 2005-2013, showing the modeled cover types for the entire patch with background RGB image for each year (1st row from the top), a closeup of the RGB image showing finer-scale vegetation structure for each year (2nd row from the top), and classified cover types for the closeup time series (3rd row).The bottom row shows (from left to right): a closeup area from a 2003 aerial image taken at the end of the fire season, dNBR for the closeup area, and dNBR for the whole patch. Although the 2003 image quality is poor, note the extensive green canopy cover that characterized this patch following fire. To highlight the principal metric used to represent the degree of delayed mortality within each patch, the percent of non-shadowed pixels comprised by mature green trees for each time step is displayed in the 1st row.

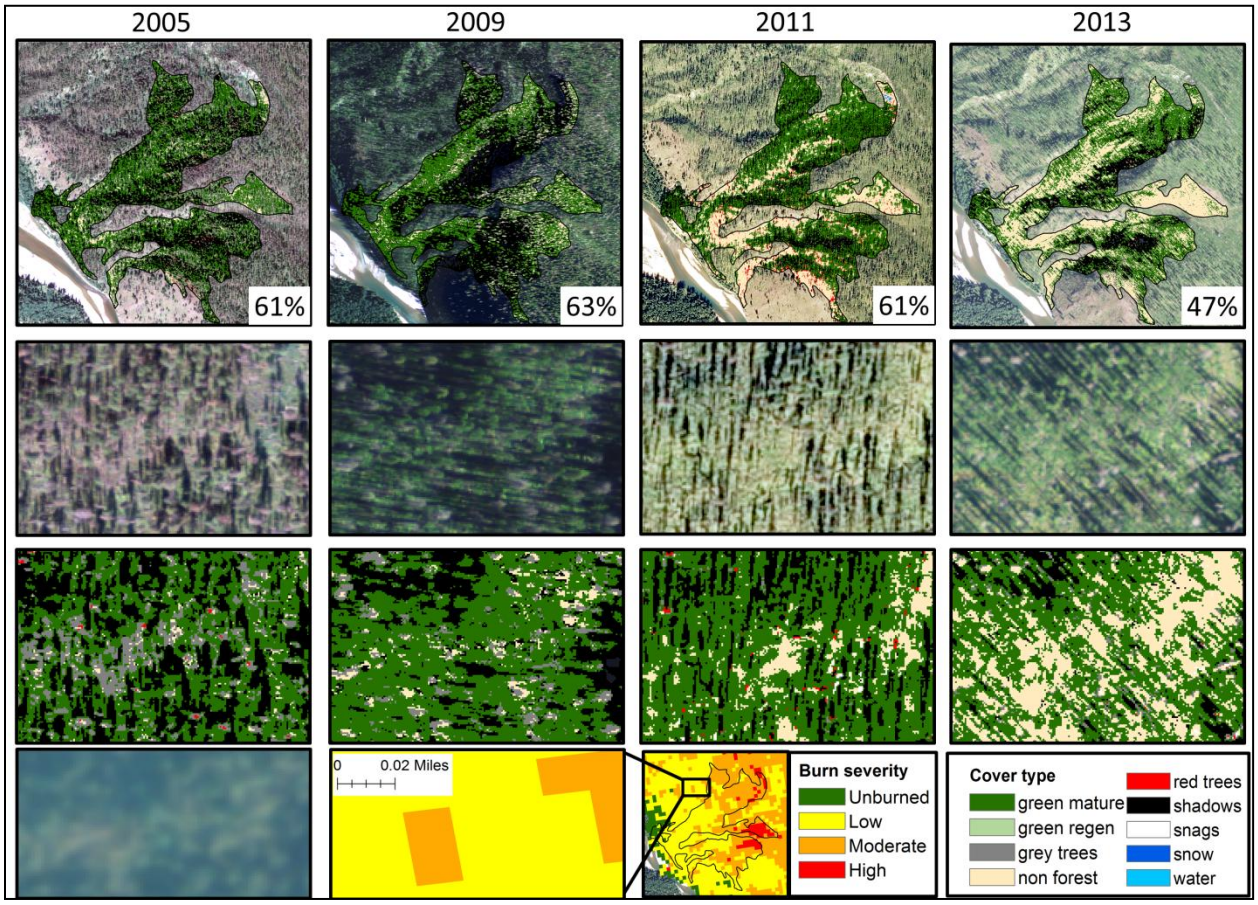

Figure 7. Notched boxplots showing the distribution of modeled mature green tree canopy cover over the 2005-2013 period for burned patches in a) all forest types pooled, b) ponderosa pine, c) Douglas-fir, d) western larch, e) lodgepole pine, f) spruce-fir, and g) cedar-hemlock forest types. Note that forest types are defined by the dominant cover species, but most patches are comprised by a mix of tree species.

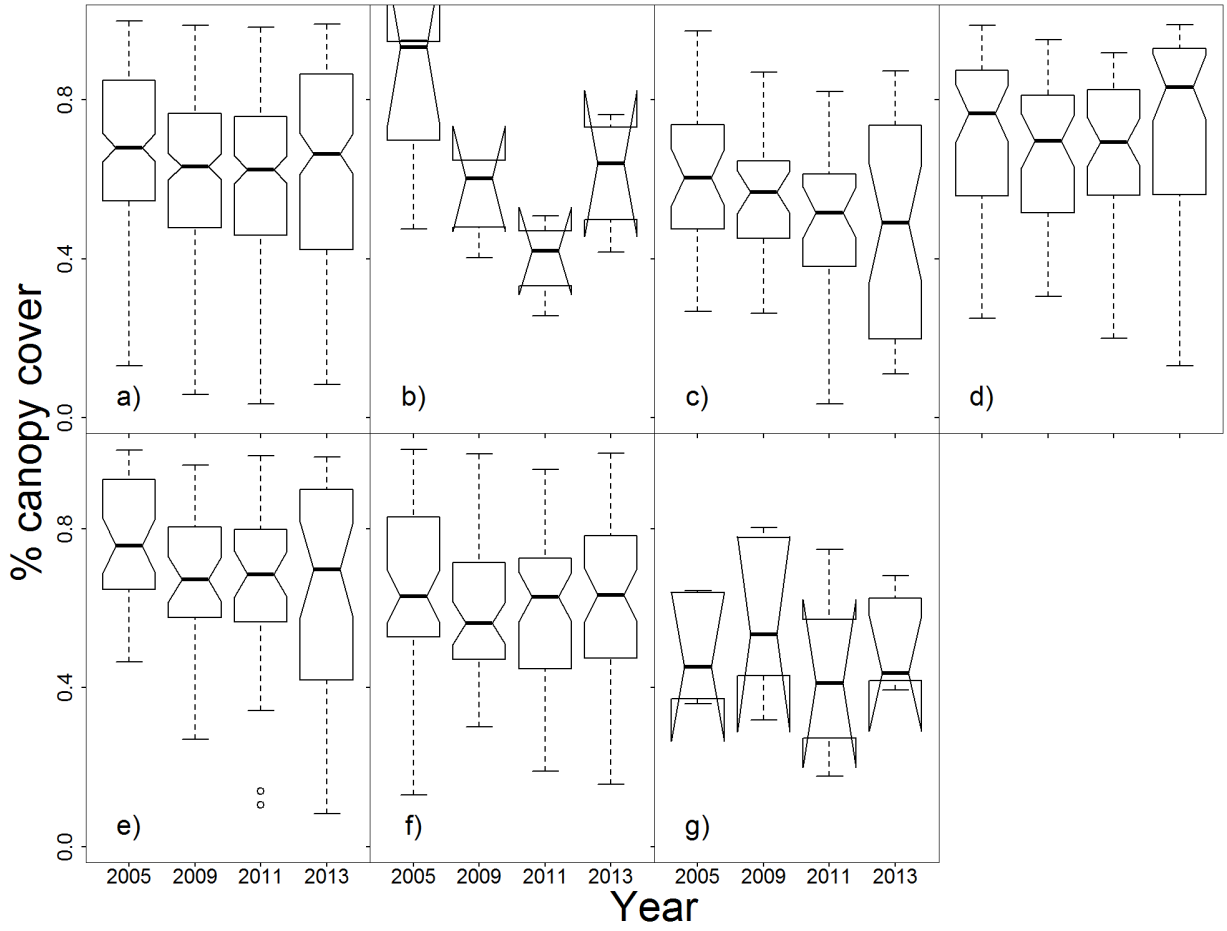

Figure 8. Notched boxplots showing the distribution of changes in modeled mature green tree canopy cover over the 2005-2013 period for unburned patches in a) all forest types pooled, b) ponderosa pine, c) Douglas-fir, d) western larch, e) lodgepole pine, f) spruce-fir, and g) cedar-hemlock forest types. Note that forest types are defined by the dominant cover species, but most patches are comprised by a mix of tree species. Dramatic changes in canopy cover as a result of delayed post-fire mortality would not be expected in these patches. Thus, they represent a type of control for comparison with burned patches.

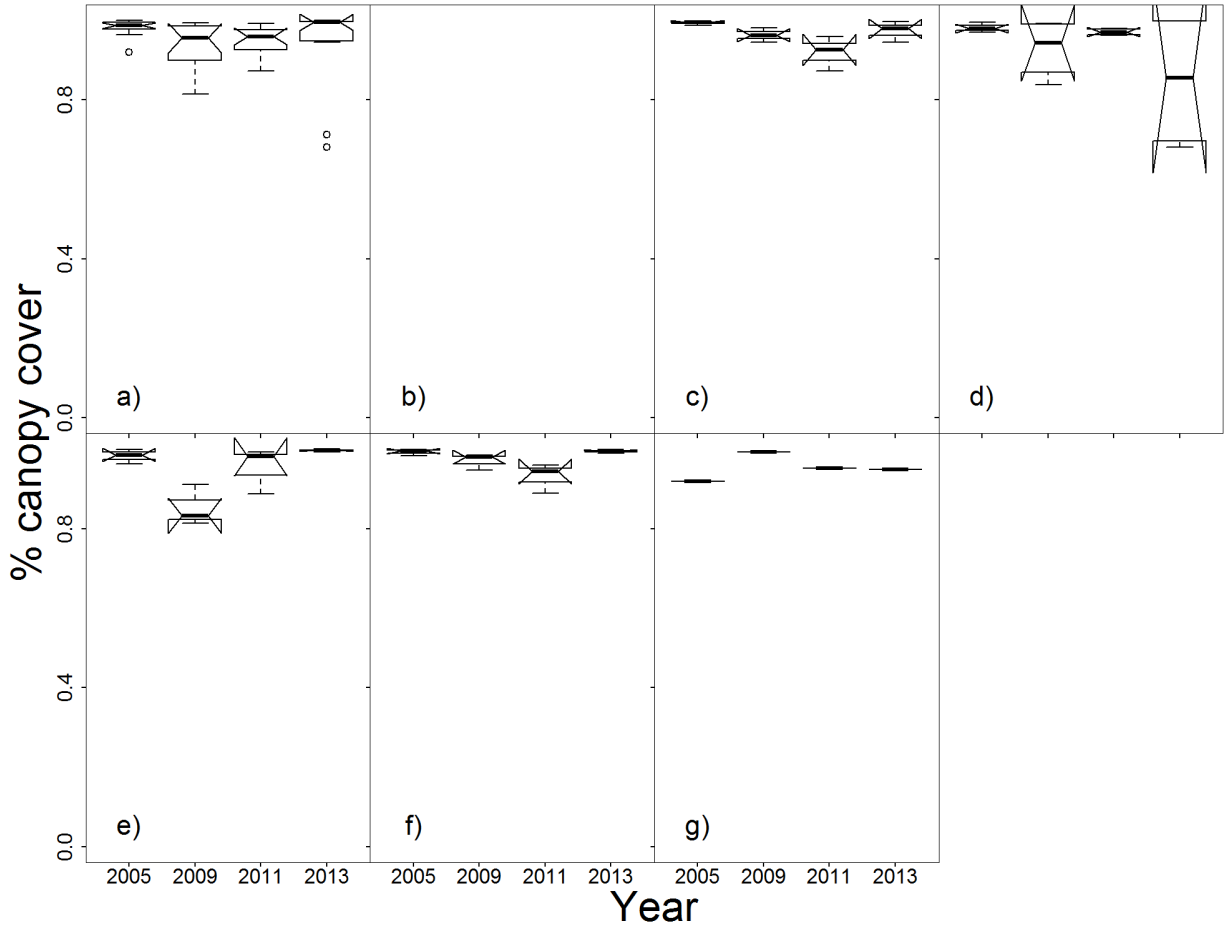

Figure 9. Notched boxplots showing the distribution of changes in modeled mature green tree canopy cover over the 2005-2013 period for burned patches within each individual fire, including: a) Anaconda Fire of 1999, b) Moose Fire of 2001, c) Roberts Fire of 2003, d) Center Mountain Fire of 2003, and e) Harrison Fire of 2003.

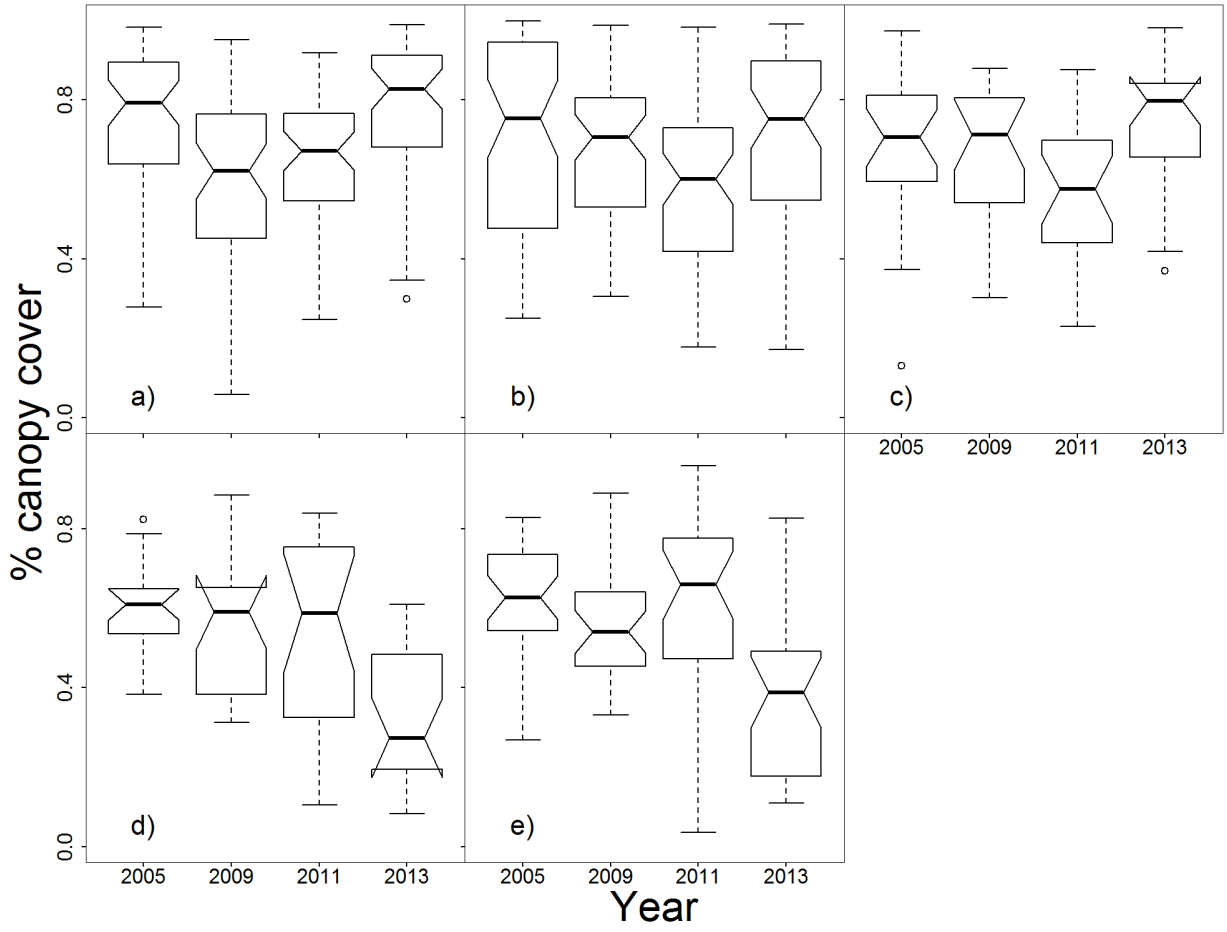

Table 1. Summary of the characteristics of fires sampled in this study and the field data collected in relation to fire characteristics.

			Fire severity (% of area)				# patches sampled			# plots sampled		
Fire Name	Fire year	Fire Size (acres)	Unburned	Low	Moderate	High	Unburned	Low	Moderate	Unburned	Low	Moderate
Anaconda	1999	11,356	20	39	34	7	0	8	0	0	15	0
Moose	2001	72,666	20	37	31	11	0	5	2	0	18	4
Robert	2003	54,500	20	31	37	12	0	5	3	0	13	6
Harrison	2003	6,653	29	21	39	11	0	6	2	0	9	4
Center Mountain	2003	5,666	44	17	32	6	0	7	0	0	13	0
Unburned	NA	NA	NA	NA	NA	NA	17	0	0	34	0	0
Total							17	31	7	34	68	14

Table 2. Table listing the beetle species observed in field surveys of trees in burned and unburned plots. For each beetle species, its principal tree host species and its potential lethality (primary vs. secondary) are also listed. Primary beetles are those that are generally capable of killing live trees, whereas secondary beetles generally only kill declining trees.

Bark beetle species	Host tree species	Beetle type
Mountain pine beetle (*Dendroctonus ponderosae*)	PIPO, PICO, PIMO, PIFL	Primary
Western pine beetle (*Dendroctonus brevicomis*)	PIPO	Primary
Douglas-fir bark beetle (*Dendroctonus pseudotsugae*)	PSME	Primary
Spruce beetle (*Dendroctonus rufipennis*)	PIEN	Primary
Western Balsam Bark Beetle (*Dryocoetes confusus*)	ABLA	Primary
Cedar bark beetles (*Phloeosinus spp.*)	THPL	Primary
Pine engraver (*Ips pini*)	PIPO, PICO, PIMO, PIFL	Secondary
Emarginate Ips (*Ips emarginatus*)	PIPO, PICO, PIMO, PIFL	Secondary
Red Turpentine (*Dendroctonus valens*)	PIPO, PICO	Secondary
Douglas-fir pole beetle (*Pseudohylesinus nebulosus*)	PSME	Secondary
Douglas-fir engraver (*Scolytus unispinosus*)	PSME	Secondary
Fir engraver (*Scolytus ventralis*)	ABGR, ABLA	Secondary

Table 3. Criteria used to define tree condition, determine the timing of tree death and assign mortality agents to dead trees in the field surveys.

Mortality agent code	Mortality agent description	Evidence/criteria
PFD	Pre-fire dead tree, not beetle attacked	• Highly decayed • Few branches, little bark • No evidence of bark beetle • Charred
PFB	Pre-fire dead tree, attacked by beetles	• Fully or partially excavated beetle galleries present • Boring dust or pitch tubes likely ***not*** present or are partially burned/consumed by fire • Exit holes evident on tree bole • Exit holes may show char on inner surface • Galleries may show char or fire damage where partially exposed at time of burn
POB	Tree survived fire, killed post-fire by beetles	• Fully or partially excavated beetle galleries present • Boring dust or pitch tubes **may be** present • Exit holes evident on tree bole • Exit holes show no evidence of being burned
BBU	Tree killed by bark beetles; timing unknown	• Fully or partially excavated beetle galleries present • Exit holes evident on tree bole • Evidence of beetle attack timing too limited to tell with certainty
FKT	Fire-killed tree	• Recently dead • Char on bark, branches, or roots • Many branches and bark still present on tree • No evidence of bark beetle
LIVE	Live tree, not attacked by beetles	• Green needles present • Live cambium
UNK	Dead tree, mortality agent unknown	• Clearly not pre-fire snag • No evidence of bark beetle or fire

Table 4. (a) Summary table of the performance statistics and (b) a confusion matrix for the Random Forest models used to classify vegetation cover type. Model performance statistics are provided for models run using all years combined and for each year individually. Accuracy values are provided for the overall model performance and for each vegetation cover type individually. In (b) the confusion matrix was derived from the model for all years combined.

(a)

	Overall		Class specific accuracy								
	Accuracy	Kappa	Mature trees	Regeneration	Grey trees	Red trees	Snags	Non forest	Shadows	Snow	Water
all years combined	78.36	0.76	84.46	79.57	86.13	90.93	85.5	84.56	91.64	98.25	89.88
2005	72.93	0.7	81.21	74.12	83.7	98.73	89.15	65.81	90.34	92.02	88.73
2009	90.23	0.89	85.4	92.91	96.24	99.58	92.91	85.82	98.31	1	1
2011	78.95	0.76	77.03	94.97	89.94	86.67	88.3	96.24	96.24	98.84	92.49
2013	82.84	0.81	79.97	67.9	92.91	100	89.58	91.65	99.58	96.25	95.83

(b)

	Reference								
Prediction	Mature trees	Regeneration	Red trees	Grey trees	Snags	Non forest	Shadows	Snow	Water
Mature trees	40	17	0	3	4	3	1	0	2
Regeneration	12	37	0	4	0	14	1	0	1
Red trees	0	2	48	6	2	2	0	0	0
Grey trees	3	1	8	40	1	3	0	2	0
Snags	3	0	3	5	50	4	0	5	0
Non forest	1	1	1	1	2	33	0	0	0
Shadows	1	0	0	1	0	0	51	0	9
Snow	0	0	0	0	1	1	0	50	0
Water	0	2	0	0	0	0	6	0	48

Table 5. Summary of plot-scale field data and beetle attack observations stratified by forest cover type for both burned and unburned plots. Post-fire beetle severity is presented as the percentage of all available trees that survived fire (e.g. live trees of each species). Primary beetles are those that are capable of killing live trees, whereas secondary beetles generally only kill declining trees. A list of bark beetle species considered as primary and secondary are presented in Table 2.

	# plots sampled			% plots attacked			Post-fire beetle attack severity (% killed)			
							Primary Beetles		Secondary Beetles	
Cover type	Full	Structure	Total	All beetles	Primary Beetles	Secondary Beetles	Density	BA	Density	BA
Burned										
PIPO	11	10	21	29	10	24	31	32	19	30
LAOC	16	9	25	44	40	16	7	10	6	2
PSME	6	5	11	36	36	27	22	33	13	11
PICO	11	4	15	60	20	60	3	6	16	19
ABLA-PIEN	2	2	4	100	50	100	8	35	0	0
THPL-TSHE	5	3	8	50	38	50	3	5	7	9
Total	51	33	84							
Unburned										
PIPO	4	0	4	100	75	100	7	11	0	0
LAOC	4	0	4	100	75	75	2	4	3	3
PSME	5	2	7	86	57	57	2	5	3	2
PICO	8	0	8	63	50	25	3	3	3	5
ABLA-PIEN	4	2	6	100	100	33	3	6	1	0
THPL-TSHE	5	0	5	100	40	60	1	3	1	0
Total	30	4	34							

Table 6. Summary of the tree-level field data documenting beetle attack observations stratified by tree species. Pre- and post-fire beetle severity are presented as the percentage of all available trees that survived fire (e.g. live trees of each species). Primary beetles are those that are capable of killing live trees, whereas secondary beetles generally only kill declining trees. A list of bark beetle species considered as primary and secondary are presented in Table 2. The mean % bole attack was estimated as the average percent of bole circumference between ground level and 1.5m where bark beetle galleries were recorded. The interquartile range (IQR) is defined as the 25^{th}-75^{th} percentile of observed values.

	pre-fire beetle severity (% BA)		post-fire beetle severity (% BA)		mean % bole attack (IQR)	
Tree species	Primary beetles	% BA killed by fire	Primary beetles	Secondary beetles	Primary beetles	Secondary beetles
PIPO	0	33	0	26	0	85 (100-100)
LAOC	0	53	0	1	0	45 (33-58)
PSME	0	51	29	20	70 (50-100)	58 (23-100)
PICO	1	70	7	41	74 (70-100)	69 (50-100)
ABLA	0	94	0	63	0	20 (5-20)
PIEN	0	81	58	7	67 (35-100)	54 (26-80)
ABGR	0	32	0	79	0	76 (65-100)
THPL	0	43	4	0	75 (63-88)	0
TSHE	0	64	0	19	0	44 (8-70)
BEPA	0	92	0	0	0	0

Table 7. Climatic data for a) pre-fire, year-of-fire, one year post-fire, and 5 years post-fire climatic conditions for each of the major fire years studied and b) growing season for all years from 1999-2013, including all major fire years and years where delayed mortality was mapped. Negative PDSI values indicate drought. Mean values represent average conditions over the May-Sept. growing season, while minimum values represent the most extreme monthly conditions within each time period.

a)

	Mean PDSI				Min PDSI			
	pre-fire	year-of	post-fire	post.fire.5	pre-fire	year-of	post-fire	post.fire.5
1999	0.86	-1.075	-2.05667	-1.141	-1.48	-1.3	-2.77	-3.79
2001	-2.148	-3.128	0.471667	-0.1052	-2.77	-3.79	-0.23	-2.24
2003	0.428	-1.3	0.862	-0.2688	-0.23	-2.24	0.28	-2.65

b)

Year	Growing season average PDSI
1999	-1.08
2000	-2.15
2001	-3.13
2002	0.43
2003	-1.30
2004	0.86
2005	0.20
2006	-0.71
2007	-1.99
2008	0.30
2009	-0.69
2010	1.72
2011	1.85
2012	0.32
2013	-0.61